

Quantifying Runoff Rates for Unpaved Road Segments in Culebra, Puerto Rico

Preston McLaughlin

7 December 2018

GIS in Water Resources



Introduction

Terrigenous sediment delivery into tropical coastal waters from land development is a key stressor influencing the global decline of coral reef ecosystems, and Caribbean reefs are amongst the most affected (Gardner et al., 2003; Mora, 2008). Coral cover in the Caribbean has been reduced on average by 80% since the mid-1970's, and coral reefs that surround Puerto Rico, have been found to be among the most threatened in the world (Burke et al., 2011, Perry et al., 2013). While increases in suspended sediment is not the only factor influencing the global decline of coral, it is an important process that tends to be overshadowed by the more well known influences related to climate change. Higher turbidity of coastal waters from sediment loading rates can result in bleaching, reduced photosynthetic activity, and increased risk of disease for coral colonies (Fabricius, 2005; Risk & Edinger, 2011; Rogers, 1990). As coastal land development increases the amount of sediment entering the coasts, the impact to nearby coral reefs will most likely continue worsen with time.

For small coastal watersheds in the northeast Caribbean, unpaved roads have been shown to be the main contributor of sediment that reaches the coast (Ramos-Scharrón & LaFevor, 2016; Ramos-Scharrón & MacDonald, 2007; Ramos Scharrón, 2010). Erosion rates from unpaved roads can be orders of magnitude greater than that of the surrounding undisturbed environments, even though the road's total surface area makes up only a small fraction of the landscape (Beschta, 1978; Ziegler et al., 1999; Gucinski, 2001; Ramos-Scharrón & MacDonald, 2005). Since the 1990s, the environmental effects related to rising rates of coastal construction have gradually become more apparent on the small, yet economically important Puerto Rican island of Culebra (Hernandez-Delgado, 2017; Ramos Scharrón, Amador, & Hernandez-Delgado, 2012).

This study focuses on predicting various volumes of runoff generated from 1.1 km of unpaved road surface at different storm intensities at the study site of Punta Aloe, which is located in the southcentral region of the island. (Figure 1) Runoff rates at the road segment scale must first be calculated in order to assess the total sediment concentration being deposited into the surrounding coastal bodies of water from this surface type. In addition to improving our understanding of these roads' contribution to the total sediment yields of Culebra's watersheds, this information will also be used to determine the effectiveness of nearby sediment traps, check dams and detention ponds that are intended to capture suspended sediment being carried through overland runoff before reaching the shoreline.

Study Area

Culebra's landmass is approximately 30 km², and lies 26 km east of Puerto Rico's mainland. The topography of the island is uniformly hilly with slopes that range between 20% and 40%, and a maximum elevation of 194 meters (Gomez et al., 2014). The island was formed from volcanic activity, and is mainly composed of andesite and various other intrusive igneous rocks (Banks, 1962). Its climate is dry sub-tropical with no permanently flowing streams, and land that is generally unsuitable for agriculture. Scarcity of available water and fertile soil led Spanish colonists to predominantly use Culebra as cattle grazing pastureland during the late 19th century. Upon defeating Spain in the Spanish American War, the United States gained control of Puerto Rico, and established a dominant presence on Culebra as a naval training ground and bombing range until the 1970's. There are currently 1,818 residents residing on the island, but year-round tourism increases the average population density considerably. The entire economy of Culebra currently revolves around environmental tourism. For this project, the road within the Punta Aloe region of Culebra will be under analysis. (Figure 1)

While its physical size is quite small, this island is surrounded by some of the most pristine coral reefs in the Caribbean (García-Sais et al., 2008.; Weil, 2003). Based on the quality and diversity of coral, as well as the multiple endangered species of marine life that reside on the island, Culebra is one of only four priority coral reef management sites in Puerto Rico (Parsons, 2010). However, since the 1990s, land development has increased substantially, which is estimated to be producing the highest sediment yields in Culebra's history (Hernandez-Delgado et al., 2017; Otaño-Cruz et al., 2017). Long-term monitoring efforts at Culebra's Canal Luis Peña Natural Reserve have discovered a 50-80% reduction in live coral cover since 1997 (Hernández-delgado et al., 2006). A combination of unpaved road segments that have up to 40% slopes, and few barriers to capture eroded sediment before being deposited directly into the sea, Culebra's surrounding corals are at an elevated risk of unhealthy sediment exposure. Sediment accumulation

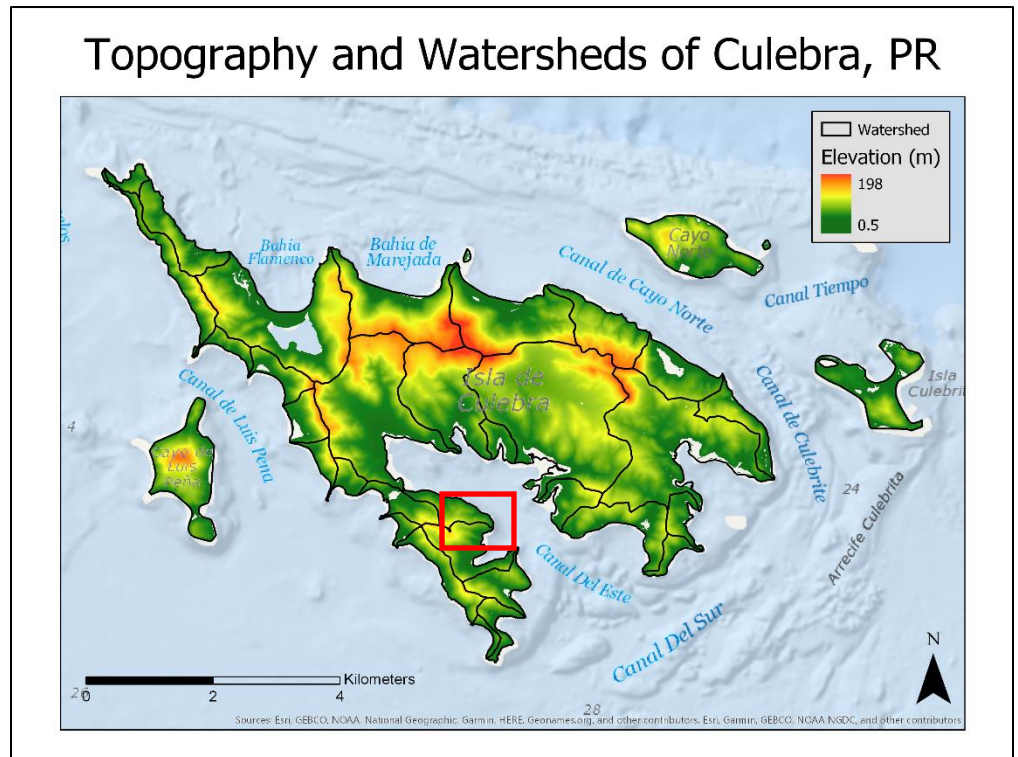


Figure 1: Red box indicates the study area of Punta Aloe

rates for near-shore reefs along the west coast of Culebra varied from 0.15 to 37 mg cm⁻² d⁻¹ between 2014 and 2015 (Otaño-Cruz et al., 2017). Any sedimentation value greater than 10 mg cm⁻² d⁻¹ is considered to be unhealthy for coral (C. S. Rogers, 1990). These values already indicate harmful amounts of sediment, which are predicted to rise with increased development and tourism. These extensive alterations to the coastal landscape have created a multitude of problems. If Culebra's surrounding corals continue to die off at its current rate, marine life will also deteriorate, which may potentially lead to a decrease in tourism and economic revenue (Hernandez-Delgado, 2012).

Field Methods

Rainfall Simulations

Rainfall simulations were used at the plot scale to quantify Horton Overland Flow (HOF) and sediment production rates. Thirty-six unpaved road simulations were carried out on slopes that ranged between 3% and 40%. 2 separate road surface types were analyzed for this project. The first type being unpaved road segments that had not been graded within 6 months of running the simulation, and the second type being unpaved road segments that had been graded within the past 6 months. The plots had an approximate area of 3 m², with a rectangular shape. At the front of the plot, smaller steel plates connected to a water collector, which contained a small opening located downslope where water samples were collected. Every minute, a runoff rate value was recorded, and suspended sediment samples were collected every 5 minutes. The rainfall simulator used a single nozzle designed to produce and distribute filtered rain shaped water droplets to the entire plot below. Six rain gauges were set around the periphery of the plot to calculate the amount of rainfall that reached the plot every 5 minutes over a 1 hour time period. The combination of averaged runoff values and averaged rainfall rates from the 6 rain gauges produced infiltration rates every 5 minutes over the course of each hour-long simulation.

Sketch Mapping and Surveying

Every road segment was mapped in as much detail as possible by hand. Every check dam and detention pond straddling the road was recorded with a GPS point, as well as a point on the map. Flow directions for each segment were also recorded so drainage points could be delineated for each section of road. In addition, the length and width were measured for every portion of road where there was a significant change in direction or topography. The slope of each segment was collected with a clinometer and stadia rod.

Rain Gauge Data

Three tipping bucket rain gauge data loggers were placed in elevated areas without canopy cover in the vicinity of each area of interest on the island. Every month, the rainfall information was collected using a HOBO® data logger. Data on the total amount of precipitation events exceeding 0.2 mm, as well as the data and duration of every storm for this project was collected over the course of 9 months. Recording began in August of 2017 and ended in May of 2018.

Recorded time intervals for each storm was set to 5-minutes in order to align with the rainfall simulation data, which was also broken up into 5-minute periods. Storm events were categorized as being any amount of rainfall over a period of time where recorded precipitation measurements had occurred within at least 1 hour of one another.

Mathematical Analysis

Infiltration Capacity Curves

As previously mentioned in the rainfall simulation section, infiltration capacity curves were generated for each of the 36 road simulations. First, the difference between collected rainfall in cm/hr for every 5-minute increment of the simulation was calculated. Then, the average runoff rate for that 5-minute period was subtracted from the rainfall rate at that time. This value indicates the infiltration capacity in cm/hr for each 5-minute period of the simulation. When all of these values are plotted against time for the entirety of the 60-minute simulation, a curved trend line is produced, which can then be used as a model for predicting rainfall infiltration over time. Horton's equation (Figure 2) was used in place of a standard statistical trendline to produce an infiltration capacity curve for every road simulation. These infiltration values would later be aggregated to create one averaged curve line.

Horton's Equation states that infiltration starts at a constant rate, and exponentially decreases with time until soil saturation reaches a certain value, and then infiltration levels off. The parameters used in Horton's Equation include the initial infiltration capacity, the final infiltration capacity, and rate of decay over time. In order to delineate the most accurate trendline possible using Horton's Equation, the Nash-Sutcliffe model efficiency coefficient (Figure 3) was specifically used instead of R^2 to determine the curve's predictive power. This coefficient was specifically created for hydrologic models. It looks at the measured mean infiltration capacities from the rainfall simulations, as well as the predicted mean infiltration capacities created from Horton's Equation, and establishes a line of best fit between both sets of data (Nash & Sutcliffe, 1970). Similar to R^2 , any value closer to 1 has a higher predictive power than values that are farther from 1. The process of finding measured and predicted infiltration capacities, and then applying a unique Nash-Sutcliffe coefficient was completed for each rainfall simulation.

$$f_{capacity} = f_c + (f_0 - f_c)e^{-t/K}$$

Figure 2: Horton's Equation

$$NSE = 1 - \frac{\sum_{t=1}^T (Q_m^t - Q_o^t)^2}{\sum_{t=1}^T (Q_o^t - \bar{Q}_o)^2}$$

Figure 3: Nash-Sutcliffe model efficiency coefficient

T-Test Analysis

After all rainfall simulations were fitted with a Nash-Sutcliffe trendline, the next step was determining if there was any statistical significance between the infiltration capacities of recently graded and ungraded road surface types. One t-test was performed to find any significance between the averaged initial infiltration capacities of all graded roads and all ungraded roads. A second t-test was used to find any significant relationship between the final infiltration capacities of graded and ungraded roads. (Figure 4) If any statistically significant relationship did exist between the two road surface types, two runoff prediction models would need to be created. If there was no significance, only one infiltration capacity curve would be needed to estimate runoff rates at different storm intensities. Based on the data, there only needed to be one model for both road surface types. Both t-tests produced p-values greater than the alpha of .05. There was a failure to reject the null hypotheses that Graded and Ungraded Initial capacities were equal, and Graded and Ungraded Final capacities were equal.

Plotting Sum Discharge Rates with Storm Intensity

By averaging the initial infiltration rates, final infiltration rates, and k values for all of the road simulations, a single infiltration capacity curve using Horton's Equation was created. All storm events that generated runoff during the 9 month period of data collection from the rain gauges were also gathered. Based on the average infiltration capacity for every 5 minute period of a storm event, and the amount of rainfall recorded every 5 minutes from the rain gauge data, total predicted runoff could be calculated. The sum precipitation minus the sum infiltration provided the sum discharge for every storm event. The total discharge and precipitation for each recorded storm event was plotted, and linear regression was used to estimate the total runoff produced from rainfall events of different intensities. (Figure 5)

F initial (cm/hr) (Graded)	F final (cm/hr) (Graded)	F initial (cm/hr) (Ungraded)	F final (cm/hr) (Ungraded)
3.7	0.8	6.2	0.8
10	0.05	8.5	0.05
6.15	0.1	11.5	0.05
5.5	0.15	31	0.04
3.3	0.5	4.1	0.6
3.6	0.32	8.4	1.2
5.6	0.4	7.1	0.6
19.5	0.05	6.3	0.8
23	0.1	6.7	0.7
9	0.1	5.3	1.4
10	1	24	0.05
16	1.1	11.2	0.04
11.5	0.6	6	1.6
8	1	18	0.05
8	0.7	7	2
		8.3	1.5
		7.5	0.05
		5	0.05
		4.5	0.3
		6.45	0.01
		6.3	0.01
Initial t-test	P value	0.989	
Final t-test	P value	0.583	

Figure 4: Initial and final infiltration capacities for every graded and ungraded road simulation, as well as the p values from both t-tests

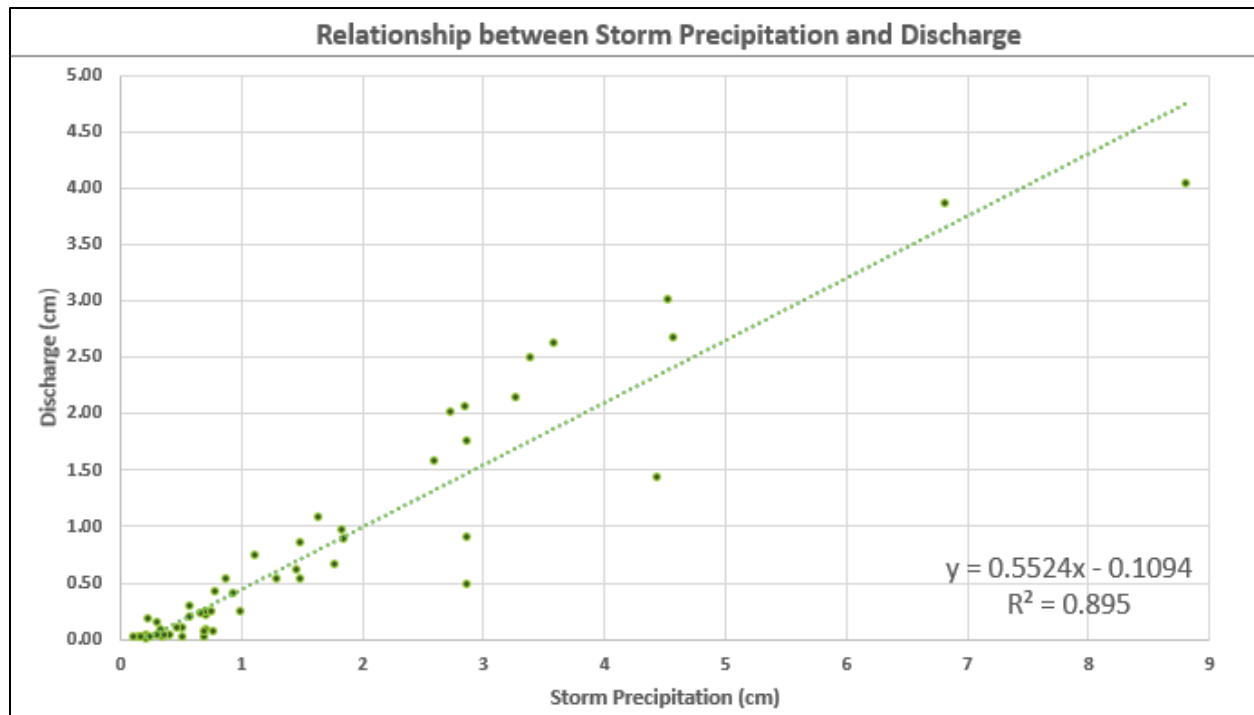


Figure 5: Graph of each runoff producing storm event and the linear regression used to predict total runoff from road segments

GIS Analysis

Downloading and Cleaning Up Data

For this project LiDAR DEM raster data with a 1 meter resolution and satellite imagery with a 10 meter resolution were used for topographic, hydrologic, digitization and visualization purposes. The downloaded datasets were too large to work with, and had to be reduced in size by using the Clip and Set Null tools. The satellite imagery raster was clipped to the extent of the watershed boundary shapefile, and all cells that had an elevation of less than .5 meters in the LiDAR DEM were removed with the Set Null function. All lake, marsh and ocean cells were removed by doing this.

Shapefiles for all unpaved roads and watershed boundaries in Culebra were downloaded as well. GPS coordinate data was uploaded to indicate areas of interest in Punta Aloe. (Figure 6) The shapefiles also needed to be cleaned up before any spatial analysis could be performed. Segments of road that did not exist anymore were removed, and watershed boundary lines that overlapped had to have their vertices snapped.

Rainfall Simulation and Sediment Trapping Structure Locations

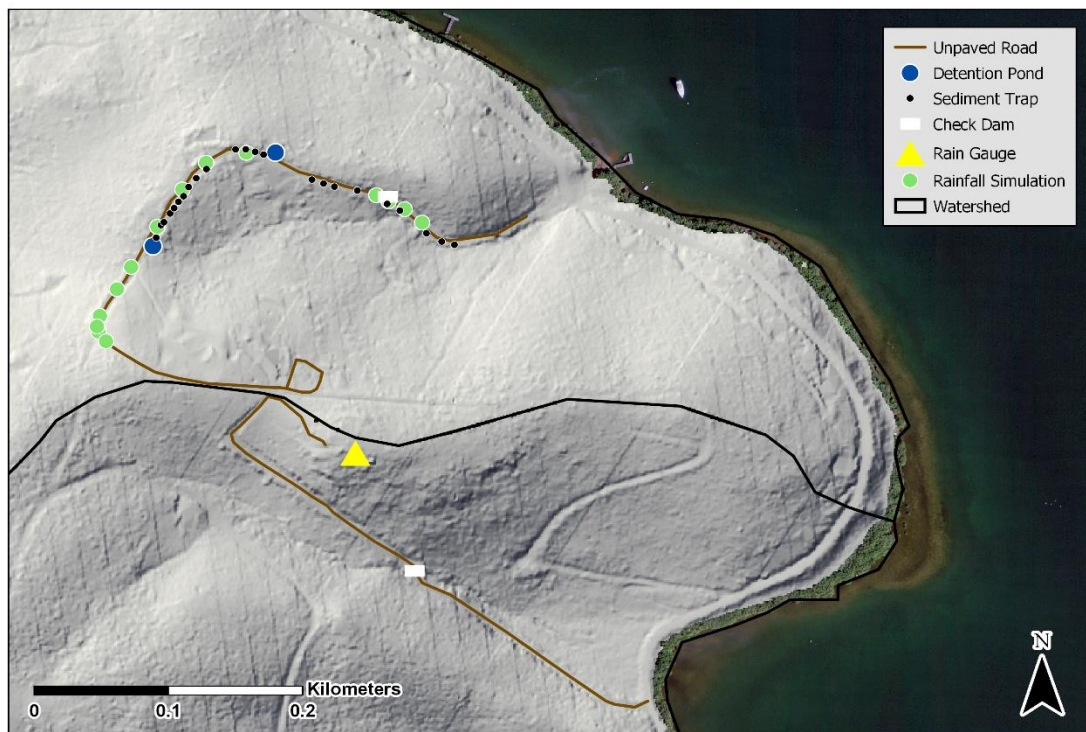


Figure 6: Reference map of rainfall simulations, sediment retention structures, and the rain gauge

Generating Stream Shapefiles from DEM Raster Data

After cleaning the DEM raster data with the “Set Null” tool, the Fill tool was then used to close any elevation gaps for proper streamflow results. “Flow Direction” was then generated using the D8 flow direction type. (Figure 7) “Flow Accumulation” followed “Flow Direction” using “Integer” output data, and a D8 flow direction type as well. Due to the high resolution of the DEM raster, many streams were initially generated with very high cell counts at the drainage points of each stream. Based on actual field observations of the ephemeral stream extents around the study area, a cell count threshold of 10,000 was used to produce stream

D8 Flow Directions for Punta Aloe with Watersheds

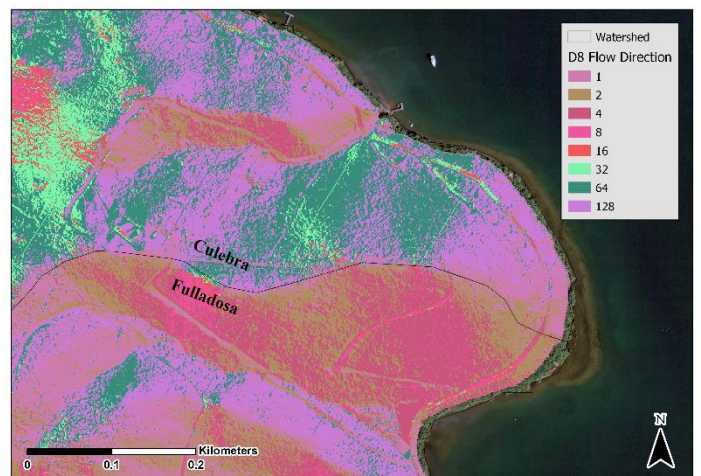


Figure 7: D8 flow direction map for Punta Aloe

segments that most closely matched the real extent of the observed streams. The “Raster Calculator” tool was used with the command “FlowAccumulation > 10,000” to designate as accurate a stream extent as possible. The last step in producing a stream shapefile was using the “Stream to Feature” tool to convert the flow accumulation raster cells to polylines. (Figure 8)

The stream segment dimensions created from this analysis will later be used in conjunction with the estimated runoff produced from the undisturbed, vegetated hillslope surfaces at different storm intensities to predict streamflow values. Unfortunately, these calculations have to wait until the undisturbed surface infiltration and runoff data is analyzed in the same way that the road surface data has been studied. Nevertheless, these stream segments generated in ArcGIS Pro are a significant first step in the right direction for future analysis.

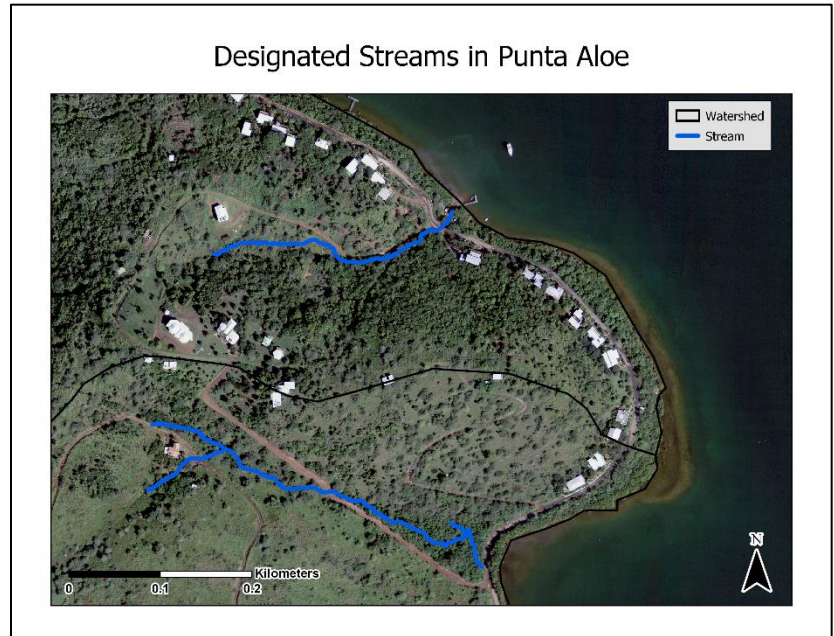


Figure 8: Finalized stream segments for Punta Aloe

Breaking the Road Polyline into Segments and Assigning a Drainage Point to Each Segment

GPS points for Punta Aloe’s detention ponds, sediment traps, check dams, and drainage points were created by using the “Excel to Table” function to convert the Latitude and Longitude coordinate spreadsheet to an attribute table in ArcGIS Pro. Once the table was uploaded, the “Display XY Data” tool was used to populate the map with all locations found within the table. The spatial locations of the detention ponds, midpoint of the V-Traps, peak of the hill, and endpoints of the road were all assigned unique drainage points. Using the “Split Line to Point” tool, each drainage point was

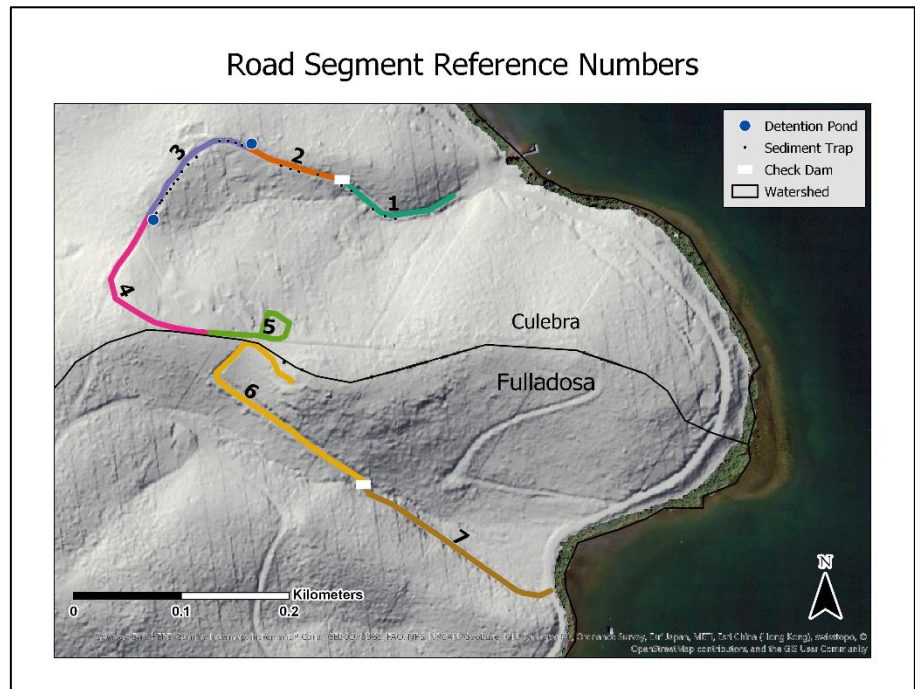


Figure 9: Road segment reference map

used as a boundary marker for the new road polylines. After running this program, 7 unique road segments were produced that would be assigned a particular volume of runoff using the linear regression model created from the rainfall simulation and rain gauge data discussed above. (Figure 9)

Calculating Runoff for Each Road and Stream Segment

The attribute table for the road segments needed to be exported into Excel for further analysis. First, a column containing an averaged road width of 4 meters was assigned to each segment. The average width was determined using the road surveying information collected in the field. Second, a group of new attribute columns were created for theoretical storm events with different intensities, ranging from 5 mm of rainfall to 40 cm of rainfall. The runoff prediction model created from the simulation and rain gauge data was then applied to every theoretical storm event to populate the new attribute columns with projected runoff volumes in cubic meters. (Figure 10) The finalized spreadsheet was exported back into ArcGIS Pro and joined with the attribute tables for the road segment and drainage point features.

For visualization purposes, the symbology was modified for both the roads and drainage points. The drainage points and road segments were assigned with graduated symbols that increased in size with increasing predicted runoff. In addition, intuitive colors that ranged from dark red to light green were given to drainage points and road segments that produced the most and the least runoff respectively. “Hillshade” was also used to produce a more detailed visual of the study area’s topography.

Results

Rainfall Simulation Curve Statistics

Based on a lack of statistical significance between graded and ungraded road surfaces in relation to infiltration capacity rates, only one model was created to predict runoff volume. Initial infiltration rate, final infiltration rate, and decay constant for all road simulations were averaged to produce one infiltration capacity curve that would be the basis for determining if the actual recorded rainfall events had theoretically produced runoff or not. The average initial infiltration capacity was 9.5 cm/hr, the average final infiltration capacity was 0.52 cm/hr, and the average decay rate was 0.13.

Every Nash-Sutcliffe model efficiency coefficient (NSE) generated for the rainfall simulation infiltration capacity curves remained greater than .68, with a number of coefficients being .99. This indicates relatively strong predictive power for all the infiltration capacity curve models that were created. The average NSE was calculated as being .76.

Runoff Producing Rainfall Events

Between August 4, 2017 and May 18, 2018, there were a total of 56 runoff producing storm events. The month of September experienced the most runoff producing events, as well as the

largest storm event. 16 runoff events were predicted as having occurred during this month. The largest storm event recorded in this dataset took place during the time Hurricane Maria swept over Puerto Rico. On September 19, 2017 8.82 cm of rainfall was recorded, and 4.02 cm of road surface runoff was generated based on the runoff model. Only 13 runoff producing storm events occurred between December 2017 and May 2018. March and April only experienced one runoff event. The smallest amount of precipitation to produce runoff occurred on October 27, when 1.2 mm of rain produced 0.2 mm of runoff. This rainfall threshold for predicted runoff production aligns almost perfectly with the minimum rainfall threshold measured for the rainfall simulations, which was 1.1 mm. Average precipitation values for the 56 rainfall events was 1.55 cm, and average discharge rates were 0.74 cm.

A positive linear association was found when total precipitation and total discharge for each runoff producing storm event was plotted. A linear regression model with an R² coefficient of 0.895 was used to predict total runoff for storm events of various intensities. The equation for this model was “y = 0.5524x – 0.1094”. For storm events that produce 4 cm of rainfall or less, there appears to be a 2:1 ratio between the amount of precipitation and the amount of runoff being produced. Total runoff begins to increase slightly more than total rainfall with storm events exceeding 4 cm. For example, a rainfall event of 2 cm is predicted as producing .995 cm or runoff, while a storm event of 10 cm is predicted to produce 5.4 cm or runoff.

Spatial Analysis using GIS

Total discharge (Q) rates in m³ were calculated when the spatial dimensions of Punta Aloe’s road segments were combined with the predicted runoff values for different storm intensities ranging from 0.5 cm (5mm) to 40 cm. (Figure 10) The maps displaying the road segments and the proportionate discharge rates at their respective drainage points provides a clear visual indication of which road segments are producing the greatest volumes of runoff. These easy to understand map graphics have the potential of being beneficial to public and private sector organizations, as well as homeowners, who are invested in minimizing the amount of suspended sediment entering Culebra’s coast by pinpointing locations that need prioritization.

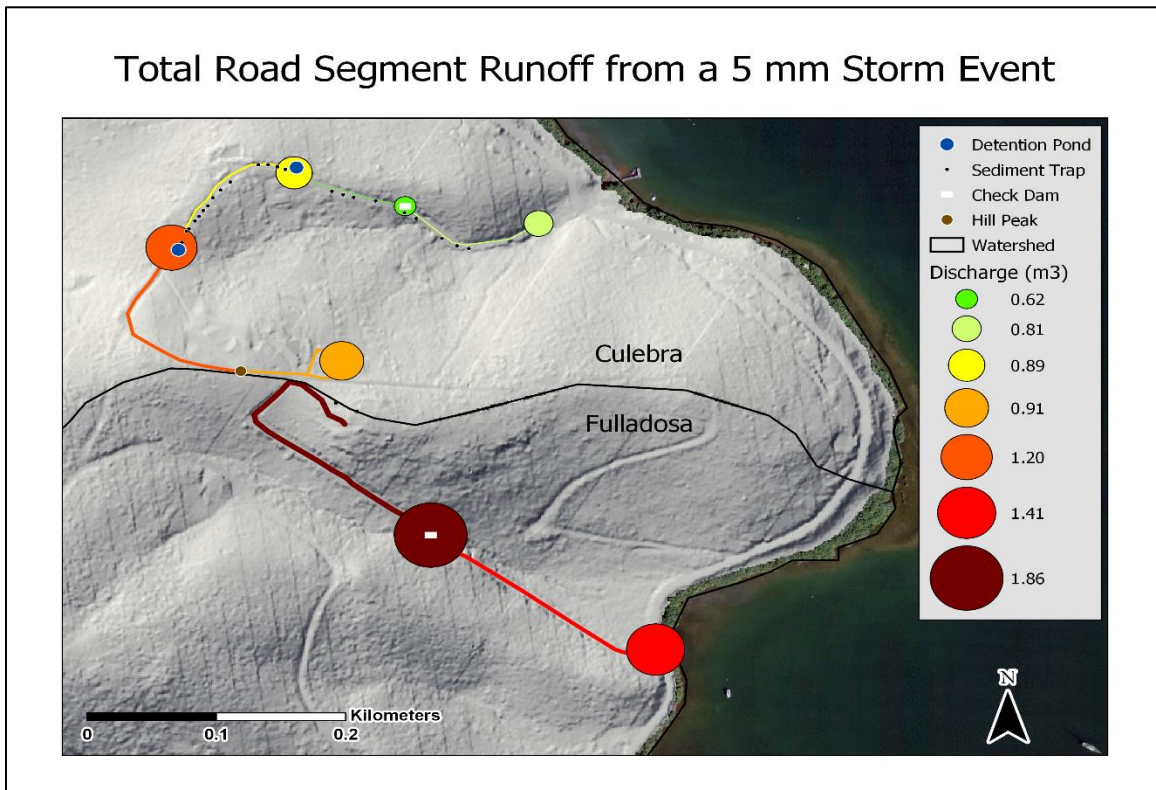
ObjectID	Length(m)	AvgWidth(m)	Q0.5 (m3)	Q1	Q1.5	Q2	Q2.5	Q3	Q3.5	Q4	Q4.5	Q5	Q5.5	Q6	Q6.5	Q7
1	119.6	4	0.81	2.12	3.44	4.76	6.08	7.40	8.73	10.05	11.37	12.69	14.01	15.33	16.65	17.98
2	91.18	4	0.62	1.62	2.62	3.63	4.64	5.65	6.65	7.66	8.67	9.67	10.68	11.69	12.70	13.70
3	132.35	4	0.90	2.35	3.81	5.27	6.73	8.19	9.66	11.12	12.58	14.04	15.51	16.97	18.43	19.89
4	176.69	4	1.20	3.13	5.08	7.04	8.99	10.94	12.89	14.84	16.80	18.75	20.70	22.65	24.60	26.56
5	134.03	4	0.91	2.38	3.86	5.34	6.82	8.30	9.78	11.26	12.74	14.22	15.70	17.18	18.66	20.14
6	274.79	4	1.87	4.87	7.91	10.94	13.98	17.01	20.05	23.08	26.12	29.16	32.19	35.23	38.26	41.30
7	208.56	4	1.42	3.67	6.01	8.34	10.59	12.93	15.18	17.52	19.85	22.11	24.44	26.78	29.03	31.35
Sum			7.73	20.13	32.72	45.32	57.83	70.42	82.94	95.53	108.13	120.64	133.24	145.83	158.34	170.92

ObjectID	Length(m)	AvgWidth(m)	Q7.5 (m3)	Q8	Q8.5	Q9	Q9.5	Q10	Q12	Q14	Q16	Q18	Q20	Q25	Q30	Q35	Q40
1	119.6	4	19.30	20.62	21.94	23.26	24.58	25.90	31.19	36.47	41.76	47.04	52.33	65.54	78.76	91.97	105.18
2	91.18	4	14.71	15.72	16.73	17.73	18.74	19.75	23.78	27.81	31.84	35.87	39.90	49.97	60.04	70.12	80.19
3	132.35	4	21.35	22.82	24.28	25.74	27.20	28.66	34.51	40.36	46.21	52.06	57.91	72.53	87.15	101.78	116.40
4	176.69	4	28.51	30.46	32.41	34.36	36.32	38.27	46.08	53.88	61.69	69.50	77.31	96.83	116.35	135.87	155.39
5	134.03	4	21.62	23.11	24.59	26.07	27.55	29.03	34.95	40.87	46.80	52.72	58.64	73.45	88.26	103.07	117.87
6	274.79	4	44.34	47.37	50.41	53.44	56.48	59.52	71.66	83.80	95.95	108.09	120.23	150.59	180.95	211.31	241.67
7	208.56	4	33.65	35.95	38.26	40.56	42.87	45.17	54.39	63.60	72.82	82.04	91.25	114.30	137.34	160.38	183.42
Sum			183.48	196.04	208.61	221.17	233.74	246.30	296.55	346.81	397.06	447.32	497.58	623.21	748.85	874.49	1000.13

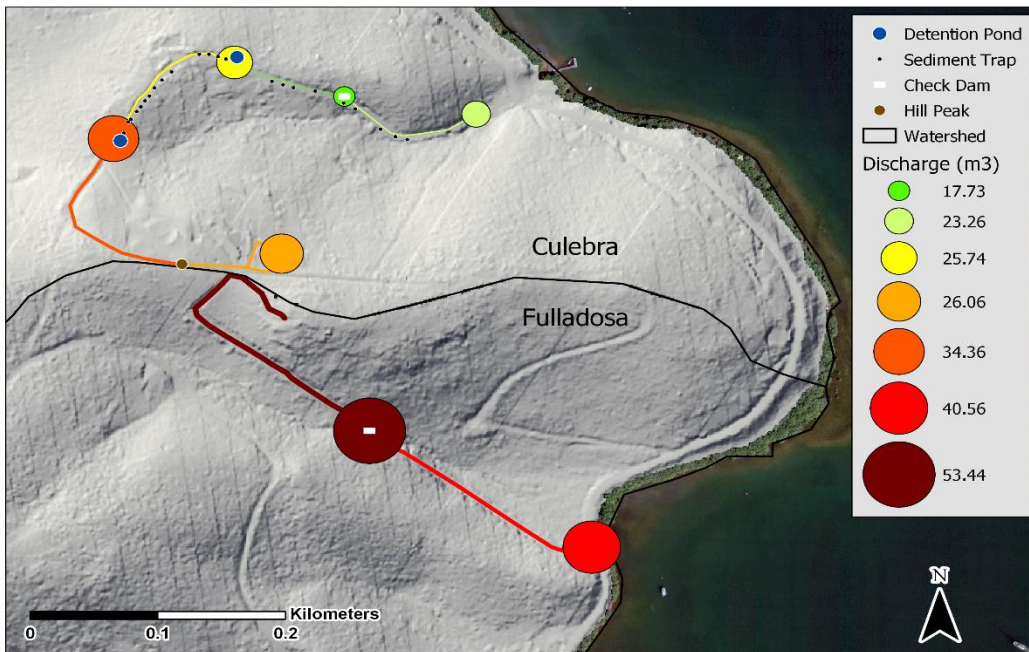
Figure 10: Tables of each road segment and their respective discharge rate in m³ for storm events that range from .5 cm to 40 cm

There is an obvious connection between the road segment's size and the volume of runoff that is predicted to be generated. (Figures 11, 12, 13) Road segments 6 and 7 (figure 9) consistently have the largest volume of runoff because of their longer lengths of 274 m and 208 m respectively, in comparison with the other segments. Of the 7.73 m³ of runoff produced from the entire road after a rainfall event of 5 mm, 3.29 m³ of that comes from segments 6 and 7 alone. In the case of a massive 40 cm storm event with 1000.13 m³ of total discharge, segments 6 and 7 would produce 425.09 m³. Road segment 2 has the smallest length at 91 meters, and was consistently predicted as producing the least runoff. For a 5 mm event, segment 2 should only be producing 0.62 m³ of discharge. For a 40 cm storm, segment 2 would be contributing 80.19 m³ to the total 1000.13 m³ of runoff.

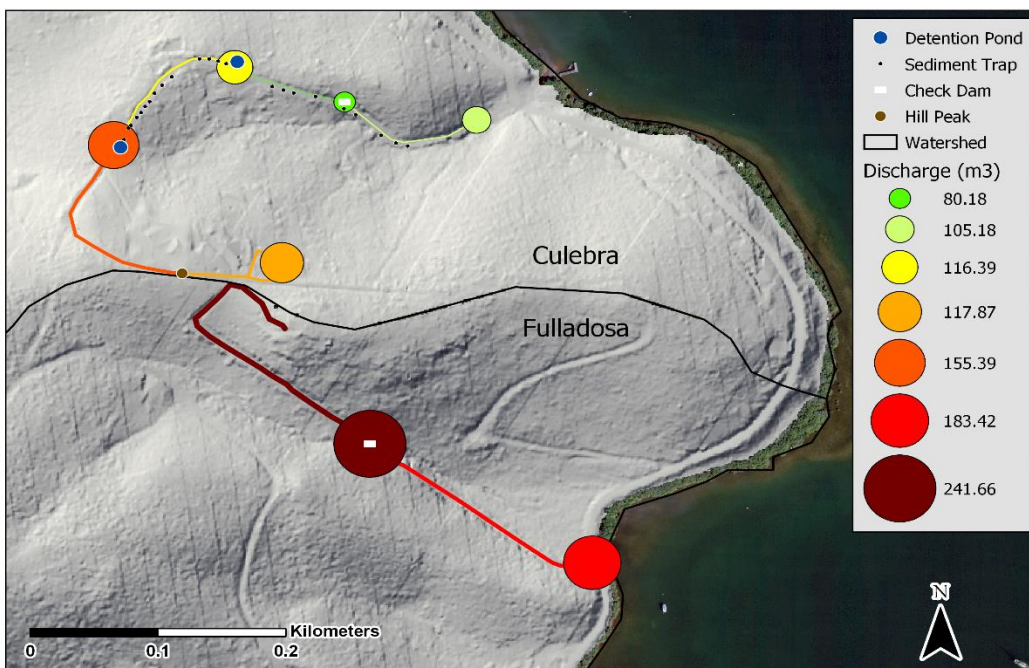
Runoff rates from these road segments can also be divided by their locations within a particular watershed. The Culebra and Fulladosa watersheds intersect with the road inside Punta Aloe. Road segments 6 and 7 are located in the Fulladosa watershed, while segments 1,2,3,4, and 5 are found in the Culebra watershed. When the road lengths of segments 6 and 7 are added together, the total predicted runoff volume produced in the Fulladosa watershed after a 5 mm storm is 3.28 m³, while segments 1,2,3,4, and 5 produce 4.45 m³ within the Culebra watershed. For the largest recorded rain gauge storm event of almost 9 cm, Fulladosa was estimated to have received 93.96 m³ of road runoff, and Culebra watershed receiving 127.12 m³ respectively. In the rare occurrence of a storm producing 40 cm of precipitation, Fulladosa watershed would receive 425 m³ of road runoff, and Culebra watershed would receive 575 m³. Approximately 42% of all total road runoff is generated from segments 6 and 7 alone.



Total Road Segment Runoff from a 9 cm Storm Event



Total Road Segment Runoff from a 40 cm Storm Event



Figures 11, 12, 13: Total estimated runoff in m³ for each road segment for a 5 mm, 9 cm, and 40 cm storm event. (Drainage point symbols remain the same, but values in key change)

Conclusions

Influxes of eroded sediment from coastal landscapes are a key stressor to the health of coral reefs located directly offshore. On the small Puerto Rican island of Culebra, continuous development and unpaved road construction have posed a serious threat to the surrounding corals for this particular reason. While there are multiple factors to take into consideration, terrigenous sediment entering coastal waters should not be disregarded by researchers and policy makers when considering ways to help improve the overall condition of corals.

The goal of this project was to quantify the volume of runoff being generated from unpaved roads in the Punta Aloe region of Culebra for storm intensities that ranged between 5 mm and 40 cm. The 1.1 km long unpaved road within Punta Aloe was chosen as the study site for this analysis. This research was also intended to determine the effectiveness of the 2 detention ponds, 23 sediment traps, and 2 check dams installed along this stretch of road.

After calculating an averaged infiltration capacity curve from every unpaved road rainfall simulation, and analyzing the rain gauge data for all 56 runoff producing storm events over the course of 9 months, linear regression was performed to produce a model with an R^2 of .895. This model estimated runoff volumes for storm events of different intensities. Through this examination, results indicated that it takes no more than 1.2 mm of rainfall to produce runoff on these unpaved road surfaces. This estimated value aligns well with the recorded minimum rainfall of 1.1 mm that was recorded during the rainfall simulations. Average total precipitation for all runoff producing storm events was 1.55 cm, and average runoff was 0.74 cm. Hurricane Maria produced the largest recorded storm event with 8.82 cm of rainfall and 4.02 cm of road runoff. The linear regression model suggests that for storm events that produce around 4 cm or less, there is a 2:1 ratio between rainfall and runoff. The amount of runoff slowly increases in relation to precipitation for storm events producing more than 4 cm of rain.

Based on the spatial analysis performed in GIS, it is clear that certain road segments in Punta Aloe need to be prioritized when developing sediment transport mitigation strategies. Road segments 6 and 7 produce the most runoff, mainly because of their long lengths. Approximately 42% of all runoff comes from these two segments that drain within the Fulladosa watershed. The remaining 58% of runoff comes from road segments 1,2,3,4 and 5, which then drain within the Culebra watershed. All but two of the sediment retention or diversion structures are found along the three road segments predicted to produce the least total runoff. In order to reduce as much runoff and transported sediment as possible being generated from roads in Punta Aloe, it is suggested that more attention be placed on the Fulladosa side of the road. Almost half of all runoff produced from this region's road comes from these 2 segments, and there is only one check dam installed to mitigate this issue.

Infiltration capacity analysis for Culebra's undisturbed, vegetated surfaces is the next step of the larger project. After this step, it will then be possible to compare the volumes of runoff created from different sources within the entire watershed. The final product of this research will

provide researchers, residents, developers and policy makers with the information necessary to help make better-informed decisions on projects aimed towards reducing the amount of terrigenous sediment making its way from unpaved roads to nearby coastal waters.

Bibliography

- Banks, T. H. (1962). Geology of Culebra Island, Puerto Rico. Retrieved from <https://scholarship.rice.edu/bitstream/handle/1911/89926/RICE0961.pdf?sequence=1>
- Beschta, R. L. (1978). Long-term patterns of sediment production following road construction and logging in the Oregon Coast Range. *Water Resources Research*, 14(6), 1011–1016. <https://doi.org/10.1029/WR014i006p01011>
- Burke, L. M., World Resources Institute., K., Spalding, M., & Perry, A. (2011). *Reefs at risk revisited*. World Resources Institute. Retrieved from <http://www.vliz.be/en/imis?refid=223234>
- Fabricius, K. E. (2005, February 1). Effects of terrestrial runoff on the ecology of corals and coral reefs: Review and synthesis. *Marine Pollution Bulletin*. Pergamon. <https://doi.org/10.1016/j.marpolbul.2004.11.028>
- Garcia-Sais, J., Appeldoorn, R., Battista, T., Bauer, L., Bruckner, A., Caldow, C., ... Williams, S. (2008). The state of coral reef ecosystems of Puerto Rico. *State of the Coral Reef Ecosystems of the United States 2008*, 75–116. Retrieved from [https://www.denix.osd.mil/denix/crid/Coral_Reef_Iniative_Database/Puerto_Rico_files/Garcia-Sais et al., 2008.pdf](https://www.denix.osd.mil/denix/crid/Coral_Reef_Iniative_Database/Puerto_Rico_files/Garcia-Sais%20et%20al.,%202008.pdf)
- Gardner, T. A., Côté, I. M., Gill, J. A., Grant, A., & Watkinson, A. R. (2003). Long-term region-wide declines in Caribbean corals. *Science (New York, N.Y.)*, 301(5635), 958–60. <https://doi.org/10.1126/science.1086050>
- Gómez-Gómez, F., Rodríguez-Martínez, J., & Santiago, M. (2014). Hydrogeology of Puerto Rico and the Outlying Islands of Vieques, Culebra, and Mona. *Scientific Investigations Map 3296*. [https://doi.org/Scientific Investigations Map 3296](https://doi.org/Scientific%20Investigations%20Map%203296)
- Gucinski, H. (2001). *Forest roads: a synthesis of scientific information*. Retrieved from <https://books.google.com/books?hl=en&lr=&id=uUNh8Moz9zUC&oi=fnd&pg=PA1&dq=Gucinski+et+al.+2001&ots=8Sbu8gJWdJ&sig=6ODwGsZnH9L9cXwZbwzk0FA3Vkg>
- Hernandez-Delgado, E., ... J. M.-M.-E., & 2017, undefined. (n.d.). Unsustainable Land Use, Sediment-Laden Runoff, and Chronic Raw Sewage Offset the Benefits of Coral Reef Ecosystems in a No-Take Marine Protected Area. *Macrothink.org*. Retrieved from <http://www.macrothink.org/journal/index.php/emsd/article/view/10687>
- Hernández-Delgado, E. A., Ramos-Scharrón, C. E., Guerrero-Pérez, C. R. ., Lucking, M. A., Laureano, R., Méndez-Lázaro, P. A. ., & Meléndez-Díaz, J. O. (2012). Long-Term Impacts of Non-Sustainable Tourism and Urban Development in Small Tropical Islands Coastal Habitats in a Changing Climate : Lessons Learned from Puerto Rico. In *Visions for Global Tourism Industry - Creating and Sustaining Competitive Strategies* (pp. 357–398). Retrieved from <https://www.intechopen.com/download/pdf/35534>

- Hernández-delgado, E. A., Rosado, B. J., & Sabat, A. M. (2006). Management Failures and Coral Decline Threatens Fish Functional Groups Recovery Patterns in the Luis Peña Channel No-take Natural Reserve , Culebra Island , Puerto Rico La A Pérdida de Corales y la Ausencia de Cumplimiento Amenazan los Patrones de Recuper. In *Proceeding of the 57th Gulf and Caribbean Fisheries Institute* (pp. 577–606). Retrieved from http://aquaticcommons.org/13898/1/gcfi_57-41.pdf
- Mora, C. (2008). A clear human footprint in the coral reefs of the Caribbean. *Proceedings of the Royal Society B: Biological Sciences*, 275(1636), 767–773. <https://doi.org/10.1098/rspb.2007.1472>
- Nash, J. E., & Sutcliffe, J. V. (1970). River flow forecasting through conceptual models part I - A discussion of principles. *Journal of Hydrology*, 10(3), 282–290. [https://doi.org/10.1016/0022-1694\(70\)90255-6](https://doi.org/10.1016/0022-1694(70)90255-6)
- Otaño-Cruz, A., Montañez-Acuña, A. A., Torres-López, V., Hernández-Figueroa, E. M., & Hernández-Delgado, E. A. (2017). Effects of Changing Weather, Oceanographic Conditions, and Land Uses on Spatio-Temporal Variation of Sedimentation Dynamics along Near-Shore Coral Reefs. *Frontiers in Marine Science*, 4. <https://doi.org/10.3389/fmars.2017.00249>
- Parsons, T. (2010). Puerto Rico’s coral reef management priorities. Retrieved from <https://repository.library.noaa.gov/view/noaa/646>
- Perry, C. T., Murphy, G. N., Kench, P. S., Smithers, S. G., Edinger, E. N., Steneck, R. S., & Mumby, P. J. (2013). Caribbean-wide decline in carbonate production threatens coral reef growth. *Nature Communications*, 4, 1402. <https://doi.org/10.1038/ncomms2409>
- Ramos-Scharrón, C. E., & LaFevor, M. C. (2016). The role of unpaved roads as active source areas of precipitation excess in small watersheds drained by ephemeral streams in the Northeastern Caribbean. *Journal of Hydrology*, 533, 168–179. <https://doi.org/10.1016/j.jhydrol.2015.11.051>
- Ramos-Scharrón, C. E., & MacDonald, L. H. (2005, September 1). Measurement and prediction of sediment production from unpaved roads, St John, US Virgin Islands. *Earth Surface Processes and Landforms*. John Wiley & Sons, Ltd. <https://doi.org/10.1002/esp.1201>
- Ramos-Scharrón, C. E., & MacDonald, L. H. (2007). Runoff and suspended sediment yields from an unpaved road segment, St John, US Virgin Islands. *Hydrological Processes*, 21(1), 35–50. <https://doi.org/10.1002/hyp.6175>
- Ramos Scharrón, C. E. (2010). Sediment production from unpaved roads in a sub-tropical dry setting — Southwestern Puerto Rico. *CATENA*, 82(3), 146–158. <https://doi.org/10.1016/J.CATENA.2010.06.001>
- Ramos Scharrón, C. E., Amador, J. M., & Hernandez-Delgado, E. A. (2012). An Interdisciplinary Erosion Mitigation Approach for Coral Reef Protection – A Case Study from the Eastern Caribbean. *Marine Ecosystems*, 127–160. Retrieved from <http://www.intechopen.com/books/marine-ecosystems>
- Risk, M. J., & Edinger, E. (2011). Impacts of Sediment on Coral Reefs. In *Encyclopedia of*

Modern Coral Reefs (pp. 575–612). Springer, Dordrecht. <https://doi.org/10.1007/978-90-481-2639-2>

Rogers, C. (2009). Coral bleaching and disease should not be underestimated as causes of Caribbean coral reef decline. *Proceedings. Biological Sciences*, 276(1655), 197-8-200. <https://doi.org/10.1098/rspb.2008.0606>

Rogers, C. S. (1990). Responses of coral reefs and reef organisms to sedimentation. *Marine Ecology Progress Series*, 62, 185–202. <https://doi.org/10.3354/meps062185>

Weil, E., ... E. H.-D.-... A. of the U., & 2003, undefined. (n.d.). Distribution and status of Acroporid coral (Scleractinia) populations in Puerto Rico. *Researchgate.net*. Retrieved from https://www.researchgate.net/profile/Mark_Chiappone/publication/237298112_Acropora_Corals_in_Florida_Status_Trends_Conservation_and_Prospects_for_Recovery/links/0046352ec2c1c1d6af000000/Acropora-Corals-in-Florida-Status-Trends-Conservation-and-Prospects-for-Recovery.pdf#page=78

Ziegler, A. D., Sutherland, R. A., & Giambelluca, T. W. (2000). Runoff generation and sediment transport on unpaved roads, paths, and agricultural land surfaces in northern Thailand. *Earth Surface Processes and Landforms*, 25(5), 519–534. [https://doi.org/10.1002/\(SICI\)1096-9837\(200005\)25:5<519::AID-ESP80>3.0.CO;2-T](https://doi.org/10.1002/(SICI)1096-9837(200005)25:5<519::AID-ESP80>3.0.CO;2-T)